

Is a simple model based on two mixing reservoirs able to reproduce the intra-annual dynamics of DOC and NO₃ stream concentrations in an agricultural headwater catchment?

Strohmenger, L.; Fovet, O.; Hrachowitz, M.; Salmon-Monviola, J.; Gascuel-Oudou, C.

DOI

[10.1016/j.scitotenv.2021.148715](https://doi.org/10.1016/j.scitotenv.2021.148715)

Publication date

2021

Document Version

Final published version

Published in

Science of the Total Environment

Citation (APA)

Strohmenger, L., Fovet, O., Hrachowitz, M., Salmon-Monviola, J., & Gascuel-Oudou, C. (2021). Is a simple model based on two mixing reservoirs able to reproduce the intra-annual dynamics of DOC and NO₃ stream concentrations in an agricultural headwater catchment? *Science of the Total Environment*, 794, Article 148715. <https://doi.org/10.1016/j.scitotenv.2021.148715>

Important note

To cite this publication, please use the final published version (if applicable). Please check the document version above.

Copyright

Other than for strictly personal use, it is not permitted to download, forward or distribute the text or part of it, without the consent of the author(s) and/or copyright holder(s), unless the work is under an open content license such as Creative Commons.

Takedown policy

Please contact us and provide details if you believe this document breaches copyrights. We will remove access to the work immediately and investigate your claim.

Green Open Access added to TU Delft Institutional Repository

'You share, we take care!' - Taverne project

<https://www.openaccess.nl/en/you-share-we-take-care>

Otherwise as indicated in the copyright section: the publisher is the copyright holder of this work and the author uses the Dutch legislation to make this work public.



Is a simple model based on two mixing reservoirs able to reproduce the intra-annual dynamics of DOC and NO₃ stream concentrations in an agricultural headwater catchment?



L. Strohmenger^{a,*}, O. Fovet^a, M. Hrachowitz^b, J. Salmon-Monviola^a, C. Gascuel-Oudou^a

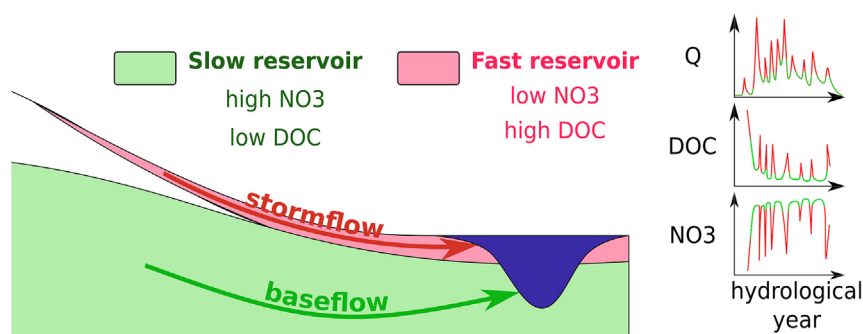
^a UMR SAS, INRAE, Institut Agro, 35000 Rennes, France

^b Department of Water Management, Faculty of Civil Engineering and Geosciences, Delft University of Technology, Delft, Netherlands

HIGHLIGHTS

- Use of stream concentrations to improve the plausibility of hydrological model.
- Simple conceptual-reservoir model to reproduce water, DOC and NO₃ pathways.
- Transport through groundwater and the wetland drive DOC and NO₃ dynamics.
- Sources of stream DOC and NO₃ are the fast and slow reservoir, respectively.

GRAPHICAL ABSTRACT



ARTICLE INFO

Article history:

Received 11 March 2021

Received in revised form 8 June 2021

Accepted 23 June 2021

Available online 26 June 2021

Editor: Ouyang Wei

Keywords:

Parsimonious model

Water quality

Stream

Agricultural catchment

Climate

Seasonality

ABSTRACT

Agriculture disturbs the biogeochemical cycles of major elements, which alters the elemental stoichiometry of surface stream waters, with potential impacts on their ecosystems. However, models of catchment hydrology and water quality remain relatively disconnected, even though the observation that dissolved organic carbon (DOC) and nitrate (NO₃⁻) have opposite spatial and temporal patterns seems relevant for improving our representation of hydrological transport pathways within catchments. We tested the ability of a parsimonious model to simultaneously reproduce intra-annual dynamics of stream flow, DOC and NO₃⁻ concentrations using 15 years of daily data from a small headwater agricultural catchment (AgrHyS observatory). The model consists of an unsaturated reservoir, a slow reservoir representing the groundwater and a fast reservoir representing the riparian zone and preferential flow paths. The sources of DOC and NO₃⁻ are assumed to behave as infinite pools with a fixed concentration in each reservoir that contributes to the stream. Stream concentrations thus result from simple mixing of slow and fast reservoir contributions. The model simultaneously reproduced annual and storm-event dynamics of discharge, DOC and NO₃⁻ concentrations in the stream, with calibration KGE scores of 0.77, 0.64 and 0.58 respectively, and validation KGE scores of 0.72, 0.58 and 0.43 respectively. These results suggest that the dynamics of these concentrations can be explained by hydrological transport processes and thus by temporally variable contributions from slow (NO₃⁻ rich and DOC poor) and fast reservoirs (DOC rich and NO₃⁻ poor), with a poor representation of the biogeochemical transformations. Unexpectedly, using the concentration time series to calibrate the model increased uncertainty in the parameters that control hydrological fluxes of the model. The legacy storage of NO₃⁻ resulting from agricultural history in the studied catchment supports the assumption that the main DOC and NO₃⁻ sources behave as infinite pools at the scale of several years. Nevertheless, reproducing the long-term trends in solute concentration would require additional information about DOC and NO₃⁻ trends within the reservoirs.

© 2021 Elsevier B.V. All rights reserved.

* Corresponding author.

E-mail address: Lstrohmenger@unistra.fr (L. Strohmenger).

1. Introduction

Stream solutes concentrations result from complex interactions among the physiographic characteristics of a catchment, anthropogenic and hydroclimatic conditions, biogeochemical processes and hydrological connectivity (Basu et al., 2010; Davis et al., 2014; Dick et al., 2014). Past intensification of agriculture during the 20th century resulted in large nutrient legacy pools in many agricultural catchments (Basu et al., 2011; Haygarth et al., 2014; Hrachowitz et al., 2015; Dupas et al., 2018) and associated nutrient export to surface water in Europe (Bouraoui and Grizzetti, 2011; Howden et al., 2011; Graeber et al., 2012) and elsewhere (Alexander and Smith, 2006; Bartsch et al., 2013; Smith et al., 2013). Such exports can alter the stoichiometry and lead to degradation of the quality of water bodies (Lee et al., 2000; Borah et al., 2002; Fuß et al., 2017). Reducing nutrient transfer from land to stream requires knowledge about their sources, and transport and transformation processes (Pettersson et al., 2001; Ford et al., 2018; Dusek et al., 2019).

Models can be used to test hypotheses about physical and biogeochemical processes that govern the transfer and transformation of water and solutes (Pettersson et al., 2001; Birkel et al., 2017; Dusek et al., 2019; Trevisan et al., 2019). Because internal states of a catchment cannot be observed directly and hydro-chemical properties cannot be measured everywhere, at least some model parameters need to be calibrated using metrics that compare model outputs to observed time series (Hrachowitz and Clark, 2017). Calibrating parameters with stream concentration time series along with stream flow may improve the physical plausibility of hydrological models because of the biogeochemical and hydrological constraints that need to be reproduced (Pettersson et al., 2001; Medici et al., 2012; Hrachowitz et al., 2013a; Woodward et al., 2013; Fovet et al., 2015; Birkel et al., 2017).

Conceptual-type process-based models often distinguish three water storage components within a catchment – surface, vadose and groundwater hydrology – each of which is associated with a water flow path: preferential, shallow and groundwater flow, respectively (e.g. Addiscott and Mirza (1998)). Water in these components differs in its solutes concentrations, flow velocity and associated transit times (e.g. Aubert et al. (2013)). Thus, the relative water flux contributions of multiple individual flow paths influence the chemical composition of a river (Woodward and Stenger, 2018). These relative contributions vary in time (Hrachowitz et al., 2013b) depending upon precipitation and catchment wetness state, which influences intra-annual variations (seasonal, storm and inter-storm conditions) of solute concentration in the river (Zuocco et al., 2016). Using time series of multiple elements has the potential to provide further insights into the relative contributions of individual flow components and the dynamics of different water flow paths. Therefore, they could also increase the confidence in a model's parameters and physical plausibility. This is particularly true if the solutes spatial distribution and stream concentration dynamics differ greatly (Shrestha et al., 2013; Woodward and Stenger, 2018; Shafii et al., 2019), as is frequently observed for dissolved organic carbon (DOC) and nitrate (NO_3^-) (Taylor and Townsend, 2010).

Previous studies showed that seasonal variation in DOC and NO_3^- are closely related to water table fluctuations in groundwater-fed catchments (Aubert et al., 2013; Thomas et al., 2016; Abbott et al., 2018; Strohmenger et al., 2020). In contrast, short-term variations in DOC and NO_3^- have been connected to the activation of subsurface and surface flow paths during storm events and the subsequent hydrological connection of DOC-rich and NO_3^- -poor riparian soils to the stream, especially for near-surface soil layers (Bernal et al., 2002; Outram et al., 2014; Bowes et al., 2015; Fovet et al., 2018a; Strohmenger et al., 2020).

Several process-based models, including SWAT (Arnold et al., 1998), TNT2 (Beaujouan et al., 2002), INCA (Whitehead et al., 1998), and HYPE (Lindström et al., 2010) emphasize on biogeochemical processes to reproduce both DOC and NO_3^- stream concentration dynamics (Hrachowitz et al., 2016). These models differ in their representation

of multiple biogeochemical processes that control DOC and NO_3^- (see e.g. Ferrant et al. (2011)) and usually simulate DOC and NO_3^- separately in distinct routines or even in different versions of the model, which leads to different representations of each element and, finally, to a distinct calibration of hydrological and biogeochemical parameters. Such (semi-)distributed approaches allow land management scenarios to be compared, since they explicitly represent spatial dynamics of a solute within the catchment due to differences in land use, agricultural practices or climate conditions on medium-to-large catchment areas. As Beven (2001) highlighted, each spatial unit (grid cell or hydrological response unit) in distributed models can have a different parameter value, which means that many of them must be specified (Kelleher et al., 2017). The limited amount of information available in observed data sets to quantify these parameters leads to equifinality (Beven and Binley, 1992; Beven and Freer, 2001). To limit these disadvantages, there have been recent efforts to design models that build increasingly integrated representations of catchment processes to simultaneously reproduce the hydrological response and dynamics of solutes concentrations. By reducing the number of required parameters controlling spatial resolution and process complexity (i.e. the degree of freedom), while still exploiting the utility of observations of multiple solutes for parameterizing models, these approaches have been shown to reduce equifinality and thereby increase the consistency and physical plausibility of models. For example, Xu et al. (2012), Seibert et al. (2009) and Musolff et al. (2016) expressed loads of DOC, total organic carbon or NO_3^- as a function of groundwater storage only. Similarly, Birkel et al. (2014), Fovet et al. (2015) and Woodward and Stenger (2018) successfully applied catchment-scale conceptual models to simulate stream loads of either DOC or NO_3^- . Using such parsimonious approach for simultaneous modelling of DOC and NO_3^- is an opportunity to provide new insights on water pathways in catchment and their role on river water quality, but, to our knowledge, no previous study simulated NO_3^- and DOC by an integrative representation of various flow pathways.

The objective of this study was therefore to develop an integrated process-based conceptual-type model able to simultaneously reproduce hydrological and multiple hydro-chemical stream signatures, such as seasonal and storm-event dynamics of stream flow, DOC and NO_3^- stream concentrations at a daily time step. More specifically, we tested the following hypotheses:

- i) The model can simultaneously reproduce these intra-annual dynamics of DOC and NO_3^- stream concentrations based only on mixing temporally varying contributions from functionally distinct systems and thus model components, which suggests that hydrological transport is the dominant control of stream solute dynamics.
- ii) Hydrological parameter values and uncertainties differ when calibrating a hydrological model using only stream flow and when calibrating a hydro-chemical model using both stream flow and concentrations, since concentration time series parameterize the model better.

This study contributes to more integrated understanding of catchments and constitutes an initial step in strengthening the connection between catchment-scale hydrology models and water quality models.

2. Methods

2.1. Study site

The Kervidy-Naizin catchment is located in the Brittany region of western France (48°N, 2°5'W; Fig. 1) and forms part of the AgrHyS Critical Zone Observatory (Fovet et al., 2018b). This 5 km² headwater catchment is dominated by intensive agricultural activities. Land use is characterized by intensive mixed crop-livestock farming, with maize (36% of area), cereals (32%) and grasslands (13%), and high indoor livestock (dairy production, indoor pig breeding and poultry) density

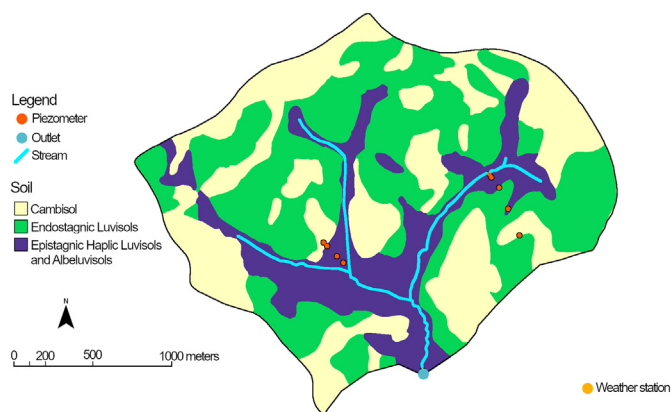


Fig. 1. Map of the Kervidy-Naizin catchment (Brittany, France). Cambisols are well-drained soils, Endostagnic Luvisols are moderately well-drained, and Epistagnic Haplic Luvisols and Albeluvisols are poorly drained (FAO classification (WRB, 2006)).

of five livestock units ha^{-1} (Viaud et al., 2018; Casal et al., 2019b; Casal et al., 2019a). The topography is relatively flat, and the elevation ranges from 98 to 140 m above sea level. Soils have a silty loam texture and are well drained Cambisols in the upslope domain and poorly-drained Epistagnic Haplic Luvisols and Albeluvisols in the downslope riparian domain (Fig. 1, FAO classification (WRB, 2006)). The underlying parent material is a variety of Brioverian schists of low permeability, and above it lies a fissured and fractured weathered layer 1–30 m deep (Molénat et al., 2005). The climate is temperate oceanic, with a mean (\pm standard deviation) annual temperature of 11.2 ± 0.6 °C. Mean annual precipitation reaches 810 ± 180 mm yr^{-1} . The catchment is drained by a second-Strahler-order intermittent stream that frequently dries up from July–October and has mean runoff of 296 ± 150 mm yr^{-1} .

During the 1970s, the intensified agricultural production led to excessive N inputs (Cheverry, 1998) that have been reduced by environmental policies following the 1990s (Casal et al., 2019b). In this landscape, most DOC and NO_3^- accumulate in wetland soils and groundwater, respectively (Aubert et al., 2013; Strohmenger et al., 2020).

2.2. Data monitoring

We used daily aggregated meteorological and stream flow measurements collected from 2002 to 2017. Precipitation, air temperature, global radiation and wind speed were recorded hourly by a weather station (Cimel Enerco 516i) located 1 km east of the outlet. Potential evapotranspiration (PET) was calculated using the Penman equation (Penman, 1956). Stream level was recorded at the outlet of the catchment every minute by a float-operated shaft-encoder level sensor (Thalimedes OTT), then converted to stream flow using a rating curve (Carlier, 1998).

Stream water was sampled manually each day at ca. 17:00 at the outlet station. Samples were filtered in the field (pore size: $0.22 \mu\text{m}$) and stored in the dark at 4 °C in propylene bottles. Analyses were performed within two weeks of sampling. NO_3^- concentrations were measured by ionic chromatography (DIONEX DX 100, ISO 10304 (1995), precision: 2.5%). DOC was estimated as total dissolved carbon minus dissolved inorganic carbon using a carbon analyzer (Shimadzu TOC 5050A, Petitjean et al. (2004), precision for DOC: 0.7 mg l^{-1}).

3. Model description

3.1.1. Model structure

We used a simple semi-distributed hydrological model based on the FLEX model family (Fenicia et al., 2006; Fenicia et al., 2014) to represent the hydrological system. We chose the model structure according to the approach of Hrachowitz et al. (2014). The model structure selected (Fig. 2) is a customized version of the M6 model from Hrachowitz

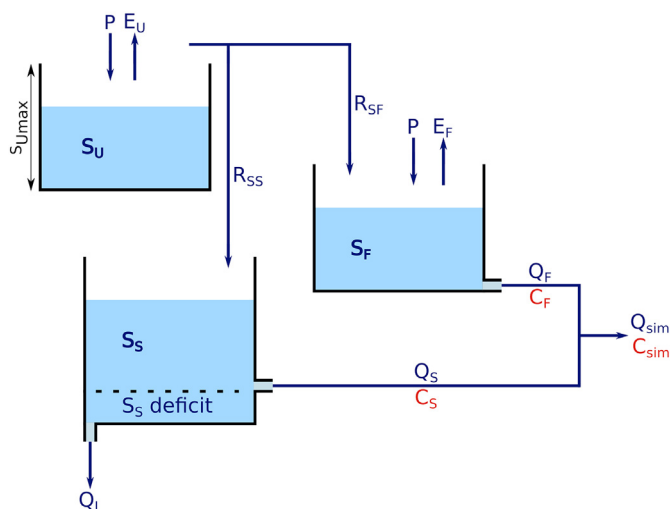


Fig. 2. Conceptual diagram of the hydro-chemical model. P is precipitation, E_i , S_i and Q_i are the i th reservoir's evaporative fluxes, water storage and contributions to the modeled discharge Q_{sim} , respectively. $S_{U\text{max}}$ is the storage capacity of the unsaturated reservoir, and R_{SS} and R_{SF} are water flows from S_U to S_S and S_F , respectively. Q_S and Q_F are the slow and fast contributions to stream flow, respectively. Q_L are deep losses. C_S , C_F and C_{sim} are the solute concentrations of Q_S , Q_F and Q_{sim} , respectively.

et al. (2014). It comprises three reservoirs, similar to those in the conceptual model of Birkel et al. (2010): unsaturated (S_U), slow-responder (S_S) and fast-responder (S_F). Conceptually, the S_U , S_S and S_F reservoirs represent the unsaturated root-zone of the hillslopes, the groundwater and the riparian compartments within the catchment, respectively. Water fluxes via the S_F reservoir are interpreted as preferential and overland flows (Q_F and R_{SF}), the flux from S_U to S_S represents infiltration and groundwater recharge (R_{SS}), and the flux from S_S to the stream is the base flow sustained by shallow groundwater (Q_S).

The rainfall-runoff model (Fig. 2) uses daily rainfall P [mm d^{-1}] and PET [mm d^{-1}] to simulate daily specific discharge at the outlet Q_{sim} [mm d^{-1}]. The unsaturated reservoir S_U receives water from rainfall (Table 1, Eq. (6)). The runoff coefficient (Cr) depends on the volume of water currently stored in S_U (Table 1, Eq. (1)).

Water that cannot be held in S_U (R_u , Table 1, Eq. (2)) is redistributed according to the splitter C_p between the S_F (C_p) and S_S ($1-C_p$) reservoirs (Table 1, Eqs. (3) and (4)). The remaining water in S_U is available for transpiration (E_U , Table 1, Eq. (5)).

The slow reservoir S_S is recharged by R_{SS} (Table 1, Eq. (8)). This S_S reservoir slowly drains into the stream flow according to a linear storage-discharge relationship that is controlled by parameter k_S proportionally to its area $1-f$, when the current S_S water storage is positive (Table 1, Eq. (7)). During the simulation, the S_S reservoir can have a storage deficit (Fig. 2), which must be filled to enable activation of slow flow from S_S to reproduce the no-flow period at the outlet in summer. We attributed a constant draining flow from the S_S reservoir as calibration parameter Q_L (Fig. 2), which reproduces the deep losses from shallow groundwater (Table 1, Eq. (8)).

The fast reservoir S_F receives water from S_U and direct rainfall (Table 1, Eq. (12)). S_F rapidly drains into the stream according to a linear storage-discharge relationship that is controlled by parameter k_F , proportionally to its area f (Table 1, Eq. (10)). The remaining water in the S_F reservoir is available for transpiration (E_F , Table 1, Eq. (11)). Total simulated stream discharge equals the sum of slow and fast contributions from S_S and S_F , respectively (Table 1, Eq. (14)).

3.2. Chemical model

One objective of the study was to assess whether a simple model based on hydrological contributions and two different sources of the solutes could reproduce the temporal patterns of stream DOC and

Table 1
Water balance, state and flux equations of the model. See Table 2 for a description of the parameters.

Reservoir	Process	Equation	Unit	
Unsaturated	Runoff coefficient	$Cr = \left(\frac{S_U}{S_{Umax}}\right)^{10^{Cr}} \leq 1$	-	(1)
	Runoff	$Ru = CrP$	mm d ⁻¹	(2)
	Runoff from S _U to S _F	$R_{SF} = RuCp \frac{1-f}{f}$	mm d ⁻¹	(3)
	Recharge from S _U to S _S	$R_{SS} = Ru(1 - Cp)$	mm d ⁻¹	(4)
	Evaporation	$E_U = \begin{cases} \text{Pet}, \text{Pet} < S_U \\ S_U, \text{Pet} \geq S_U \end{cases}$	mm d ⁻¹	(5)
Slow	Water balance	$dS_U/dt = P - Ru - E_U$	mm d ⁻¹	(6)
	Slow flow	$Q_S = k_S S_S (1 - f) \geq 0$	mm d ⁻¹	(7)
	Water balance	$dS_S/dt = R_{SS} - Q_S - Q_L$	mm d ⁻¹	(8)
Fast	Solute flux to stream	$F_S = Q_S C_S$	mg d ⁻¹	(9)
	Fast flow	$Q_F = k_F S_F f$	mm d ⁻¹	(10)
	Evaporation	$E_F = \begin{cases} \text{Pet}, \text{Pet} < S_F \\ S_F, \text{Pet} \geq S_F \end{cases}$	mm d ⁻¹	(11)
	Water balance	$dS_F/dt = P + R_{SF} - E_F - Q_F$	mm d ⁻¹	(12)
Stream	Solute flux to stream	$F_F = Q_F C_F$	mg d ⁻¹	(13)
	Total discharge	$Q_{sim} = Q_S + Q_F$	mm d ⁻¹	(14)
	Solute concentration	$C_{sim} = \frac{F_S + F_F}{Q_S + Q_F}$	mg l ⁻¹	(15)

NO_3^- concentrations. We therefore assumed that the fast and slow reservoirs are the main sources of DOC and NO_3^- , respectively. The fast reservoir represents flow paths in riparian soils, which have been identified as the main source of stream water DOC and contribute mainly during storm events (Morel et al., 2009; Lambert et al., 2014). The slow reservoir represents the shallow groundwater, which receives NO_3^- leached from the unsaturated reservoir and contributes subsurface water to the stream that sustain the base flow and export of NO_3^- (Molénat et al., 2008; Aubert et al., 2013). Thus, we set different and fixed DOC and NO_3^- concentrations in the S_F and S_S reservoirs (C_S and C_F, Fig. 2), so that there was no need to specify the concentration in S_U. By using fixed concentrations, we assumed that both reservoirs acted like infinite pools of solutes. Because of the larger supply of DOC from riparian organic soils (Lambert et al., 2013; Humbert et al., 2015) and the legacy mass storage of NO_3^- connected to the stream via groundwater (Molénat et al., 2008; Basu et al., 2010), these compartments may indeed behave like an infinite source of DOC and NO_3^- , respectively, over the time scales of model application in this study. We defined the prior range of values of solute concentrations (maximum concentration of 39.5 and 124.4 mg l⁻¹ for DOC and NO_3^- , respectively) based on the observed 2002–2017 time series (Table 2).

The daily stream concentration of a solute (C_{sim}, Fig. 2) thus results exclusively from the complete mixing of two end members: slow and fast flow components (Table 1, Eqs. (9), (13) and (15)). We assumed no additional in-stream processes because we had no information with which to evaluate them or to distinguish them from mixing

processes. This assumption seemed reasonable since the study site is a small headwater catchment with a short stream distance (<2 km) and thus negligible in-stream routing times (Morel et al., 2009).

3.3. Performance metrics and model calibration

We used the Kling-Gupta efficiency score (KGE, Gupta et al. (2009)) to assess the goodness of fit between simulated and observed times (Eq. (16)). As stated by Knoben et al. (2019), KGE > -0.41 indicates “good” model, while KGE < -0.41 indicates “poor” models performance.

$$KGE = 1 - \sqrt{(r-1)^2 + (\alpha-1)^2 + (\beta-1)^2} \quad (16)$$

$$r = \text{corr}(X_{obs}, X_{sim}) \quad \alpha = \frac{\sigma_{Xsim}}{\sigma_{Xobs}} \quad \beta = \frac{\mu_{Xsim}}{\mu_{Xobs}}$$

$$KGE_x = 1 - KGE$$

where μ and σ are the mean and standard deviation, respectively, of observed and simulated time series X, which can be stream flow or concentration variables.

KGE_x ranges from 0-infinity, and optimal parameter sets tend to minimize KGE_x scores. We assessed the overall goodness of fit (KGE_{global}) of the model as the Euclidian distance of equally weighted KGE_x scores of discharge, DOC and NO_3^- (Eq. (17)).

$$KGE_{global} = \sqrt{KGE_Q^2 + KGE_{DOC}^2 + KGE_{NO3}^2} \quad (17)$$

We used global likelihood uncertainty estimation (GLUE, Beven and Binley (1992)) to estimate parameter values and uncertainties. The calibration period was set to 2013–2017, after a 2-year initialization period, and the test period was set to 2002–2012. We performed a Monte Carlo random sampling strategy (10⁷ iterations) with uniform prior parameter distributions within given ranges based on expert knowledge and feasible limits (Table 2). The parameter sets from the prior distribution were assessed using a likelihood measure relative to the observations. We used an inverse normalized KGE_{global} so the objective function value would increase as the goodness of fit of the simulations increased (Eq. (18)).

$$OF^i = \frac{\sum_n KGE_x^n}{KGE_x^i} \quad (18)$$

Table 2
Uniform prior distributions and descriptions of the parameters of the hydro-chemical model.

Parameter	Prior range of the parameter	Unit	Description
S _{Umax}	1.0 700	mm	Maximum storage of the unsaturated reservoir
Cru	-1.0 1.0	-	Control of runoff generation
Cp	0.0 1.0	-	Ratio of runoff flux to the fast reservoir
k _S	0.0 0.1	d ⁻¹	Storage coefficient of the slow reservoir
k _F	0.1 1.0	d ⁻¹	Storage coefficient of the fast reservoir
Q _L	0.0 1.5	mm d ⁻¹	Deep losses from the slow reservoir
f	0.0 0.3	-	Proportional area of the riparian zone in the catchment
DOC _S	0 30	mg l ⁻¹	DOC concentration in the slow reservoir
NO ₃ _S	0 100	mg l ⁻¹	NO ₃ ⁻ concentration in the slow reservoir
DOC _F	0 30	mg l ⁻¹	DOC concentration in the fast reservoir
NO ₃ _F	0 100	mg l ⁻¹	NO ₃ ⁻ concentration in the fast reservoir

where OF^i is the inverse normalized KGE_x of the i th parameter set simulation, and n the total number of parameter sets used to estimate the uncertainty.

We retained the 1000 (0.01%) best simulations (i.e. with the lowest KGE_x scores) as acceptable or “behavioral” parameter sets (Beven and Freer, 2001). Calibrated values and their associated uncertainty were estimated as the median of the acceptable range and the 10th–90th quantiles, respectively. We performed this calibration twice: once for the hydrological parameters only, using KGE_Q , and once for all parameters, using KGE_{global} .

4. Results

4.1. Simulated discharge and concentrations

Overall, the model reproduced daily discharge and solute time-series well after calibration with KGE_{global} (Fig. 3). The KGE_x scores of the median simulation for the calibration and test periods were respectively 0.23 and 0.28 for KGE_Q , 0.36 and 0.42 for KGE_{DOC} , and 0.40 and 0.57 for KGE_{NO_3} . The model performed similarly during the calibration and test periods (Fig. 3), except for NO_3^- , which showed a constant bias error during the test period, with an overall underestimation of ca. 10 mg l^{-1} .

The simulated discharge reproduced well the seasonal dynamics observed during the recharge, wet and recession periods. Daily peaks of discharge associated with storm events were captured well for the wet period and slightly overestimated for the recharge and recession periods. Although the model often simulated zero discharge during the dry period, thus capturing the main feature of base flow during this period (Supplementary material S1), it also simulated flow responses after storm events while the discharge measured remained zero during this period.

The model reproduced the opposite dynamics of stream DOC and NO_3^- at seasonal and storm-event time-scales (Fig. 3). At the beginning of the hydrological year (in Autumn), median simulated DOC concentration exceeded 10 mg l^{-1} , and NO_3^- concentration laid below 40 mg l^{-1} . During the rewetting period, DOC concentration decreased to less than 5 mg l^{-1} , while NO_3^- concentration increased to more than 70 mg l^{-1} , and they remained at these levels during the wet and recession periods. At the end of the recession period, DOC concentration

increased slightly to ca. 5 mg l^{-1} , while NO_3^- concentration decreased to ca. 40 mg l^{-1} . Storm-event dynamics of the solutes were also reproduced. During storm events, DOC concentration increased by ca. 5 mg l^{-1} , and NO_3^- concentration decreased by ca. 20 mg l^{-1} , though the increases in DOC concentration were slightly underestimated at the beginning of the rewetting period and overestimated at the end of the recession period. Simulated dilution of the NO_3^- concentration during storm events was often underestimated slightly.

4.2. Hydrological vs. hydro-chemical performances

KGE_x scores were lower for simulated discharge than for simulated solute concentrations (Fig. 4): the minimum scores after 10^7 simulations were 0.05, 0.23 and 0.32 for Q , DOC and NO_3^- , respectively. The best simulations of DOC (KGE_{DOC} from 0.23–0.35) and NO_3^- (KGE_{NO_3} from 0.32–0.40) were associated with good (but not the best) simulations of discharge (KGE_Q from 0.10–1.00). As KGE_Q increased from 0.05 to 0.40, KGE_{DOC} decreased (from 0.50 to 0.23), as did KGE_{NO_3} (from 0.45 to 0.30). As KGE_Q increased from 0.50 to ca. 0.80, KGE_x scores of the solutes did not change. As KGE_Q increased above 0.80, KGE_x scores of the solutes increased. The 1000 best simulations based on the KGE_{global} (purple area, Fig. 4) were associated with a wide range of performances for simulated discharge (0.06–0.60) and solutes (0.23–0.70). The 1000 best KGE_{NO_3} were compatible with the best KGE_{DOC} (Fig. 4), while the 1000 best KGE_Q (blue area, Fig. 4) barely overlapped the 1000 best KGE_{global} simulations.

4.3. Parameter calibration

DOC concentrations in the S_S reservoir were lower than those in the S_F reservoir, with a median (10th/90th quantiles) of 1.91 ($0.36/4.66$) mg l^{-1} and 11.18 ($7.12/17.56$) mg l^{-1} , respectively (Table 3). NO_3^- concentrations in the S_S reservoir were higher than those in the S_F reservoir, with 70.82 ($48.27/90.95$) mg l^{-1} and 36.13 ($11.99/60.26$) mg l^{-1} , respectively.

Calibrating the model with the global objective function tended to yield higher uncertainties in hydrological parameters than when calibrating with the hydrological objective function (Table 3), except for

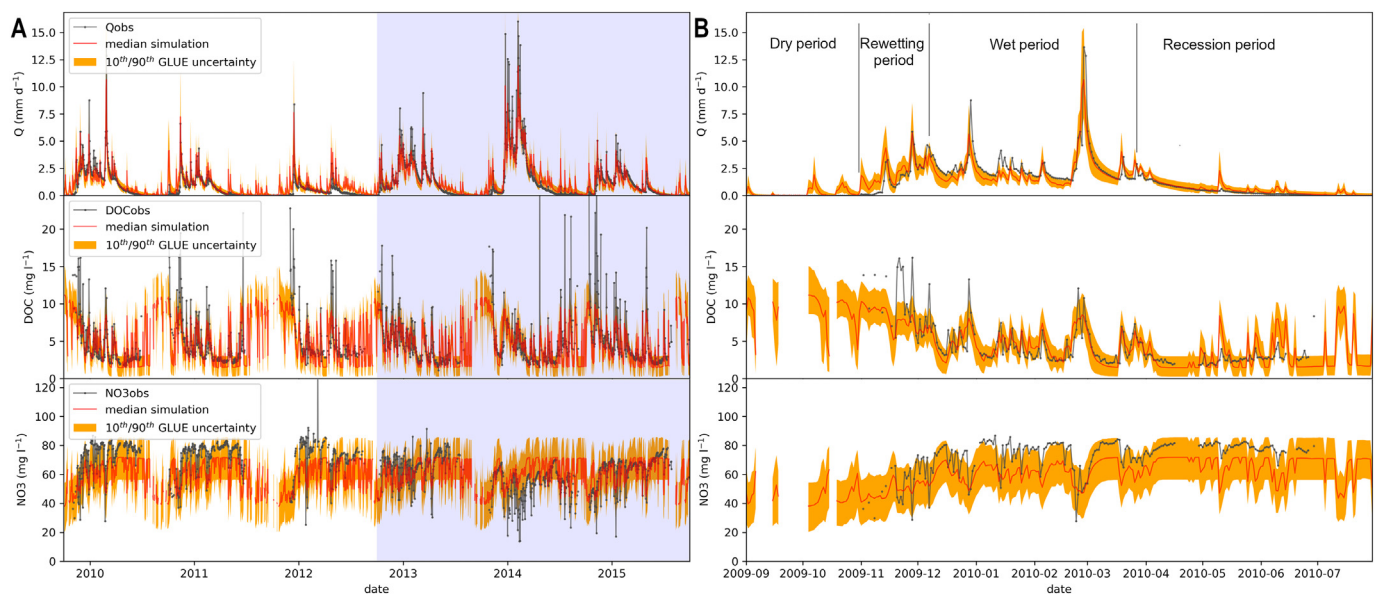


Fig. 3. Observed (gray), median (red line) and global likelihood uncertainty estimation (GLUE) (10th–90th quantiles, orange area) of the simulated times series of discharge (Q), dissolved organic carbon (DOC) and nitrate (NO_3^-) after calibration with the KGE_{global} objective function for A) the 2010–2016 period, the shaded area covers the calibration period, while the non-shaded area covers the test period, and B) one hydrological year (2010) during the validation period. (For interpretation of the references to color in this figure legend, the reader is referred to the web version of this article.)

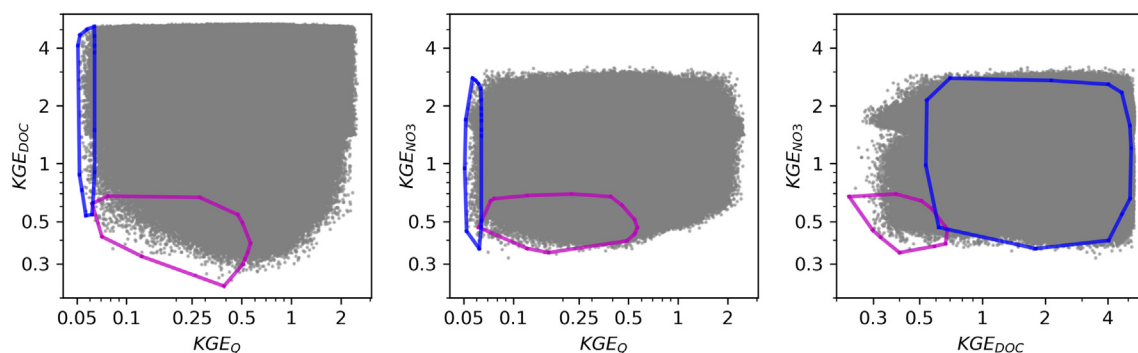


Fig. 4. Log-scaled dot-plots of KGE_x scores for discharge (Q), dissolved organic carbon (DOC) and nitrate (NO_3^-) after 10^7 simulations. The circled areas include the 1000 best simulations (i.e. with the lowest KGE_x scores) based on discharge-only (KGE_Q , blue) or overall (KGE_{global} , purple) performance metrics. (For interpretation of the references to color in this figure legend, the reader is referred to the web version of this article.)

C_p , which controls the redistribution of runoff between the riparian zone and groundwater. Calibrating the model with the global objective function also changed the median of the behavioral parameter sets (Table 3). The surface of the unsaturated zone ($1-f$) decreased slightly (i.e. surface of the riparian zone increased), while its storage capacity (S_{Umax}) increased slightly. Parameters that control the slow and fast flowrates (k_S and k_F) slightly decreased and increased, respectively. Deep losses remained almost identical for the hydrology-only and global calibrations.

4.4. Water budgets

For the 1000 best simulations based on KGE_Q only, mean simulated evaporative flux was 480 mm yr^{-1} (Fig. 5), with 463 and 17 mm yr^{-1} from the S_U and S_F reservoirs, respectively. Mean simulated annual stream flow at the outlet was 364 mm yr^{-1} , with 53% from S_S (193 mm yr^{-1}) and 47% from S_F (171 mm yr^{-1}), and annual deep losses from the S_S reservoir were ca. 57 mm yr^{-1} (15.7% of the annual stream flow).

When calibrated using the KGE_{global} , mean simulated evaporative flux was lower for S_U (404 mm yr^{-1}) and higher for S_F (24 mm yr^{-1} , Fig. 5). Stream flow increased to 403 mm yr^{-1} , with a larger contribution from S_S (227 mm yr^{-1} , 56.3%) but no change in that from S_F (176 mm yr^{-1} , 43.7%). Deep losses increased slightly to 63 mm yr^{-1} .

5. Discussion

5.1. Reproducing DOC and NO_3^- dynamics using a simple mixing model

The results suggest that a simple model with three reservoirs is a plausible conceptual model of the study catchment that simultaneously explains the seasonal, storm and inter-storm dynamics of Q, DOC and NO_3^- . The performances achieved with our model suggested that an advanced representation of biogeochemical processes is not required to

Table 3

Estimated median (and 10th–90th quantiles) of parameter values after calibration with hydrology-only (KGE_Q) and global (KGE_{global}) objective functions.

Parameter (unit)	KGE_Q	KGE_{global}
S_{Umax} (mm)	194.39 (119.29–252.43)	269.95 (81.54–503.80)
C_{ru} (–)	0.49 (0.18–0.85)	–0.05 (–0.71–0.70)
C_p (–)	0.31 (0.08–0.88)	0.23 (0.06–0.52)
k_S (d^{-1})	0.06 (0.04–0.09)	0.03 (0.01–0.08)
k_F (d^{-1})	0.24 (0.13–0.49)	0.49 (0.21–0.83)
Q_L ($mm d^{-1}$)	0.19 (0.04–0.49)	0.18 (0.03–0.61)
f (–)	0.07 (0.01–0.18)	0.12 (0.02–0.25)
DOC_S ($mg l^{-1}$)	–	1.91 (0.36–4.66)
$NO_3^-_S$ ($mg l^{-1}$)	–	70.82 (48.27–90.95)
DOC_F ($mg l^{-1}$)	–	11.18 (7.12–17.56)
$NO_3^-_F$ ($mg l^{-1}$)	–	36.13 (11.99–60.26)

capture these dynamics in the studied catchment. The main source of NO_3^- in the catchment was modeled in the slow reservoir ($160 \text{ kg-NO}_3^- \text{ ha}^{-1}$, 72% of NO_3^- export in the river), which represents the groundwater compartment, with a calibrated constant concentration of ca. 71 mg l^{-1} , while the NO_3^- concentration in the fast reservoir, which is mainly related to the riparian compartment, was calibrated to ca. 36 mg l^{-1} (Table 3). Conversely, the main source of DOC of the calibrated model was the fast reservoir ($19.7 \text{ kg-DOC ha}^{-1}$, 82% of DOC export in the river) (Morel et al., 2009; Dick et al., 2014; Casson et al., 2019), with a calibrated concentration of ca. 11 mg l^{-1} vs. ca. 2 mg l^{-1} in the S_S reservoir (Table 3). These calibrated concentrations were consistent with observed DOC and NO_3^- concentrations of 1.2 and 91.7 mg l^{-1} , respectively, in deep groundwater, and 19.8 and 6.7 mg l^{-1} , respectively, in wetlands for the 2000–2010 period in the same catchment (Aubert et al., 2013).

The large pool of NO_3^- in the groundwater originates from past and, to a lesser extent, ongoing agricultural activities in the catchment (Molénat et al., 2008; Basu et al., 2010; Aubert et al., 2013; Dupas et al., 2018; Strohmenger et al., 2020). The N legacy generated by the conversion of permanent grassland to arable land and from the massive addition of livestock slurry and manure since the intensification of agricultural in 1970–1976 (Casal et al., 2019b; Casal et al., 2019a) leached and accumulated in the vadose zone and groundwater (Cheverry, 1998; Casal et al., 2019b; Strohmenger et al., 2020). The lower NO_3^- concentration in the riparian zone is explained by the heterotrophic denitrification that can occur there under anoxic conditions when the water table reaches the soil surface (Oehler et al., 2009; Montreuil et al., 2010; Bell et al., 2015; Casson et al., 2019). Conversely, the DOC concentration measured in groundwater was low (Aubert et al., 2013), while that measured in riparian soils was high, since they have a high soil organic matter content, especially in near-surface layers, where DOC produced from decomposing microbial biomass or leaves accumulates (Morel et al., 2009; Birkel et al., 2014; Humbert et al., 2015). The differences in hydrological reactivity and chemical composition between these two conceptual reservoirs – which we equate roughly to groundwater and the riparian zone – allowed the contrasting dynamics of DOC and NO_3^- stream concentrations to be reproduced. The S_S reservoir, which is NO_3^- rich and DOC poor, contributes to the base flow, which controls seasonal concentration patterns when the water table is hydrologically connected to the stream (Supplementary material S1). The S_F reservoir, which is DOC rich and NO_3^- poor, contributes mostly during storm events, which drive rapid increases (decreases) in DOC (NO_3^-) stream concentrations, unlike inter-storm days.

Although the model reproduced seasonal and storm dynamics quite well during the test period, it always underestimated NO_3^- concentration, which had wider uncertainty intervals than discharge and DOC concentration. This underestimation was likely due to the long-term trend in NO_3^- time series. This multi-annual trend has been related to the gradual decrease in excess agricultural N that occurred mainly

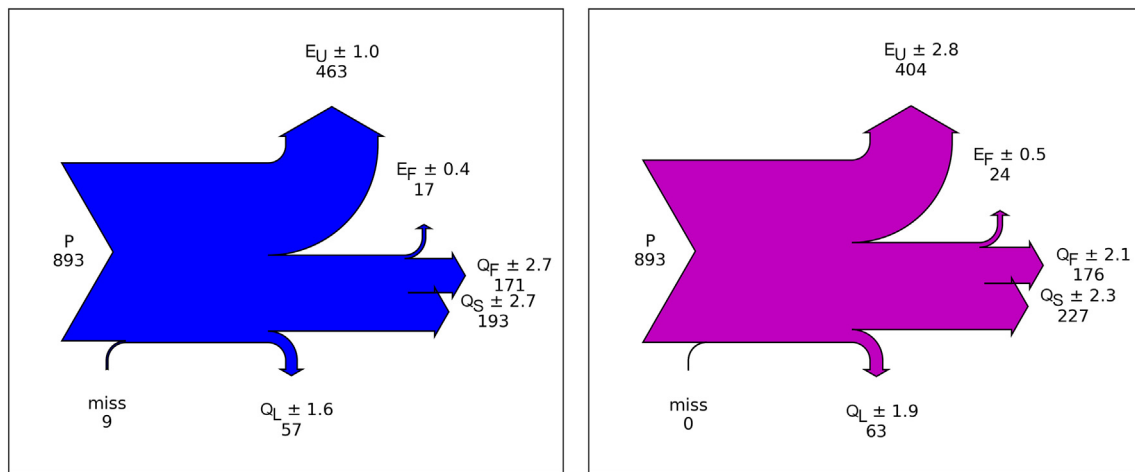


Fig. 5. Mean annual water budgets ± 1 standard error (mm yr^{-1}) for the 1000 best simulations (i.e. with the lowest KGE_x scores) based on (left) KGE_Q or (right) $\text{KGE}_{\text{global}}$. “Miss” equals total outflow minus total inflow, and may reflect storage deficit in S_S . See Table 1 for definitions.

from 1998 to 2008 and induced a slow and delayed decrease in groundwater NO_3^- concentration, and thus in stream concentrations (Dupas et al., 2018; Strohmenger et al., 2020). Since our model focused on intra-annual dynamics and assumed a constant groundwater concentration, it could not reproduce such a long-term trend. Thus, to model inter-annual dynamics of NO_3^- in the stream, those in the groundwater need to be considered, for example by a fitting a trend to S_S concentrations that would reproduce the gradual decrease in groundwater NO_3^- . Another approach would be to represent explicitly the net inputs, transport and fate of N through the three reservoirs.

Other authors also made simple mixing assumptions to model DOC at a larger scale, with a landscape-mixing model (e.g. Ågren et al. (2014)) or at similar scales (e.g. Boyer et al. (1996)). In the literature, concentrations of hydrological reservoirs were often represented as a function of temperature and water saturation, since these factors control the main biogeochemical processes that influence DOC and NO_3^- . Temperature and water saturation both increase the apparent production of DOC via solubilization and desorption (e.g. Birkel et al. (2014) and Birkel et al. (2020)) and the denitrification rate of NO_3^- (e.g. Hénault and Germon (2000)). As an initial investigation, we tested the utility of adding temperature and wetness effects, using linear functions of air temperature, reservoir storage or both, to the slow and fast reservoirs of our model, but doing so did not improve model performance ($\text{KGE}_{\text{global}}$ scores) significantly (results not shown).

5.2. The model's utility for studying climate effects on water quality

Even though the model reproduced the overall dynamics of Q, DOC and NO_3^- concentrations, it had difficulty reproducing dynamics during certain periods or successions of climatic conditions. In the case study, simulated discharge and concentrations had higher uncertainties and differed more from observations during the rewetting and recession periods than during the wet period (Fig. 3). In addition, the model overestimated NO_3^- concentrations during extreme hydrological years such as 2014. These results suggest that catchment behavior may change over time, perhaps due to pre-event hydrological conditions (Morel et al., 2009; Davis et al., 2014) or dry antecedent conditions (Outram et al., 2016). Reproducing such change in behavior over time would require information about catchment wetness.

Our results suggest that hydrological transport processes and flow paths are the main drivers of annual and storm-event dynamics of DOC and NO_3^- stream concentrations in the Kervidy-Naizin catchment. This has been reported in different catchments for other solutes, which displayed chemostatic behavior (Godsey et al., 2009; Basu et al., 2010; Basu et al., 2011). In the Kervidy-Naizin catchment, where the

riparian zone supplies a large amount of DOC and the past N surplus created a large legacy pool of NO_3^- in groundwater, the main DOC and NO_3^- sources behave as infinite pools, at least over several years. For such a near-chemostatic case, assuming constant concentrations in each reservoir seems appropriate and allows the model to test effects of precipitation regime and evaporation, and the subsequent catchment wetness and water flow paths, on the dynamics of DOC and NO_3^- concentrations in the stream. It would be interesting to test such a simple model in a gradient of catchments with diverse legacy or natural ecosystem pools (Thompson et al., 2011). Applying such a model to predict effects of climate variability on any other catchment would require testing its ability to reproduce water quality in any chemodynamic catchment.

5.3. Advantages of global calibration to better parametrize the hydrological model

The global calibration (i.e. considering in-stream concentrations (using $\text{KGE}_{\text{global}}$)), changed the distribution of simulated water flows within the catchment compared to that with the hydrological calibration (using KGE_Q). The higher medians of riparian zone area and flowrate (f and k_F , Table 3) suggest that the global calibration yielded faster flowrate in the S_F reservoir. Thus, simulations of solute dynamics were optimized with more contrasting hydrological reactivity for the S_S and S_F reservoirs. When comparing the simulations after the two calibrations, Q_F remained the same, while E_F and direct precipitation increased as f increased (Fig. 5), which implies that the S_F reservoir receives less water from the S_U reservoir. Indeed, the ratio of runoff from S_U to S_F (parameter C_p , Table 3) decreased with the global calibration. Thus, when the model was calibrated considering solute concentrations, it suggested that the hillslope contributes more to vertical flows (i.e. groundwater recharge) than horizontal flows (i.e. runoff and preferential flows) than when it was calibrated using KGE_Q . This result highlights the need to improve the representation of transit times and water flow paths. Representing and explicitly calibrating transit times within the reservoirs would be expected to improve model predictions. Rinaldo et al. (2015) developed a tool to simulate the distribution of water ages of a reservoir outflow using storage-selection functions, which have also been used successfully to simulate isotope dynamics (Harman, 2015), in-stream Cl concentration (Benettin et al., 2017) and nitrate removal peaks (Benettin et al., 2020).

Unexpectedly, parameter uncertainties (Table 3) were higher overall when calibrating with the global objective function ($\text{KGE}_{\text{global}}$) than with the hydrological objective function (KGE_Q). Thus, the simulated concentrations were less sensitive to hydrological parameters than we expected. Adding concentration time series to the objective function

led to more equifinality overall for several possible reasons: the time series of DOC and NO_3^- did not compensate for the additional degrees of freedom of the solute parameters of the hydro-chemical model, or more DOC and NO_3^- pools are necessary to reproduce catchment functioning better.

6. Conclusions

We developed a simple model to identify the main drivers of annual and storm-event DOC and NO_3^- stream concentrations in a small headwater agricultural catchment. The model consists of three reservoirs: an unsaturated reservoir representing root and vadose zones of the hill-slope, a slow reservoir representing groundwater and a fast reservoir representing the riparian zone and preferential flows. Simulated stream concentrations of DOC and NO_3^- result from the mixing of two end members: fast and slow reservoirs.

The model reasonably reproduced annual and storm-event dynamics of discharge, DOC and NO_3^- concentrations in the stream, suggesting that the main drivers of these dynamics were indeed transport processes and the differences in hydrological reactivity and chemical composition between the two contributing compartments. The main source of stream DOC was the fast reservoir, with a calibrated concentration of 11 mg l^{-1} , while the main source of stream NO_3^- was the slow reservoir, with a calibrated concentration of 71 mg l^{-1} . These constant concentrations support the idea that DOC and NO_3^- are spatially distributed in chemostatic pools (at the scale of several years) in the riparian area and groundwater, respectively, thus that an advanced representation of biogeochemical processes is not necessarily required to capture the seasonal, storm and inter-storm dynamics. Using a multi-objective function that included observed daily DOC and NO_3^- concentrations to calibrate the model led to a higher relative contribution of the slow reservoir to the stream but increased the uncertainty in the hydrological parameters, which highlight the need for additional hydrological signatures to better constrain our models. Nevertheless, reproducing the long-term trends in solute concentrations would require more information about N and C inputs or concentrations in catchment compartments. In such a chemostatic catchment, a simple model could be used to test or predict the effect of climate variability on water quality via its effect on transport processes.

Supplementary data to this article can be found online at <https://doi.org/10.1016/j.scitotenv.2021.148715>.

CRedit authorship contribution statement

L. Strohmenger: Conceptualization, Methodology, Software, Data curation, Writing – original draft, Visualization. **O. Fovet:** Conceptualization, Methodology, Validation, Investigation, Resources, Data curation, Writing – original draft. **M. Hrachowitz:** Conceptualization, Methodology, Writing – review & editing, Supervision. **J. Salmon-Monviola:** Conceptualization, Methodology, Writing – review & editing. **C. Gascuel-Oudoux:** Conceptualization, Validation, Resources, Writing – original draft, Supervision.

Declaration of competing interest

The authors declare that they have no known competing financial interests or personal relationships that could have appeared to influence the work reported in this paper.

Acknowledgments, samples and data

The French National Research Institute for Agriculture, Food and Environment (INRAE) and the Region Bretagne co-funded the doctoral program of L.S., who also received a grant for a research visit to TU Delft funded by the Université Bretagne Loire and the Region Bretagne. The AgrHyS Observatory is supported by INRAE (UMR

SAS (2010), *Observatoire de Recherche en Environnement sur les Agro-Hydrosystèmes (ORE AgrHyS)*, INRAE. <https://doi.org/10.15454/1.5499682911557678e12>). All AgrHyS data are available on the Internet: https://www6.inra.fr/ore_agrhys_eng/Data. Carbon and anion concentrations were measured at the Géosciences Rennes laboratory. We are grateful to Jean-Paul Guillard for his precious help with sampling in the Kervidy-Naizin catchment over the years and to all the farmers of Naizin-Évellys for hosting our observations, sampling and surveys.

References

- Abbott, B.W., Moatar, F., Gauthier, O., Fovet, O., Antoine, V., Ragueneau, O., 2018. Trends and seasonality of river nutrients in agricultural catchments: 18 years of weekly citizen science in France. *Sci. Total Environ.* 624, 845–858.
- Addiscott, T.M., Mirza, N.A., 1998. Modelling contaminant transport at catchment or regional scale. *Agric. Ecosyst. Environ.* 67 (2–3), 211–221.
- Ågren, A., Buffam, I., Cooper, D., Tiwari, T., Evans, C., Laudon, H., 2014. Can the heterogeneity in stream dissolved organic carbon be explained by contributing landscape elements? *Biogeosciences* 11 (4), 1199–1213.
- Alexander, R.B., Smith, R.A., 2006. Trends in the nutrient enrichment of US rivers during the late 20th century and their relation to changes in probable stream trophic conditions. *Limnol. Oceanogr.* 51 (1part2), 639–654.
- Arnold, J.G., Srinivasan, R., Muttiah, R.S., Williams, J.R., 1998. Large area hydrologic modeling and assessment part I: model development 1. *JAWRA J. Am. Water Resour. Assoc.* 34 (1), 73–89.
- Aubert, A.H., et al., 2013. Solute transport dynamics in small, shallow groundwater-dominated agricultural catchments: insights from a high-frequency, multisolute 10 yr-long monitoring study. *Hydrol. Earth Syst. Sci.* 17 (4), 1379–1391.
- Bartsch, S., Peiffer, S., Shope, C.L., Arnhold, S., Jeong, J.-J., Park, J.-H., Eum, J., Kim, B., Fleckenstein, J.H., 2013. Monsoonal-type climate or land-use management: understanding their role in the mobilization of nitrate and DOC in a mountainous catchment. *J. Hydrol.* 507, 149–162.
- Basu, N.B., et al., 2010. Nutrient loads exported from managed catchments reveal emergent biogeochemical stationarity. *Geophys. Res. Lett.* 37 (23) (n/a-n/a).
- Basu, N.B., Thompson, S.E., Rao, P.S.C., 2011. Hydrologic and biogeochemical functioning of intensively managed catchments: a synthesis of top-down analyses. *Water Resour. Res.* 47 (10).
- Beaujouan, V.R., Durand, P., Ruiz, L., Aourousseau, P., Cotteret, G., 2002. A hydrological model dedicated to topography-based simulation of nitrogen transfer and transformation: rationale and application to the geomorphology-denitrification relationship. *Hydrol. Process.* 16 (2), 493–507.
- Bell, N., Cooke, R.A., Olsen, T., David, M.B., Hudson, R., 2015. Characterizing the performance of denitrifying bioreactors during simulated subsurface drainage events. *J. Environ. Qual.* 44 (5), 1647–1656.
- Benettin, P., Soulsby, C., Birkel, C., Tetzlaff, D., Botter, G., Rinaldo, A., 2017. Using SAS functions and high-resolution isotope data to unravel travel time distributions in headwater catchments. *Water Resour. Res.* 53 (3), 1864–1878.
- Benettin, P., Fovet, O., Li, L., 2020. Nitrate removal and young stream water fractions at the catchment scale. *Hydrol. Process.* 34 (12), 2725–2738.
- Bernal, S., Butturini, A., Sabater, F., 2002. Variability of DOC and nitrate responses to storms in a small Mediterranean forested catchment. *Hydrol. Earth Syst. Sci. Discuss.* 6 (6), 1031–1041.
- Beven, K., 2001. How far can we go in distributed hydrological modelling? *Hydrol. Earth Syst. Sci.* 5 (1), 1–12.
- Beven, K., Binley, A., 1992. The future of distributed models: model calibration and uncertainty prediction. *Hydrol. Process.* 6 (3), 279–298.
- Beven, K., Freer, J., 2001. Equifinality, data assimilation, and uncertainty estimation in mechanistic modelling of complex environmental systems using the GLUE methodology. *J. Hydrol.* 249 (1–4), 11–29.
- Birkel, C., Tetzlaff, D., Dunn, S., Soulsby, C., 2010. Towards a simple dynamic process conceptualization in rainfall-runoff models using multi-criteria calibration and tracers in temperate, upland catchments. *Hydrol. Process. Int. J.* 24 (3), 260–275.
- Birkel, C., Soulsby, C., Tetzlaff, D., 2014. Integrating parsimonious models of hydrological connectivity and soil biogeochemistry to simulate stream DOC dynamics. *J. Geophys. Res.-Biogeosci.* 119 (5), 1030–1047.
- Birkel, C., Broder, T., Biester, H., 2017. Nonlinear and threshold-dominated runoff generation controls DOC export in a small peat catchment. *J. Geophys. Res.-Biogeosci.* 122 (3), 498–513.
- Birkel, C., Duvert, C., Correa, A., Munksgaard, N.C., Maher, D.T., Hutley, L.B., 2020. Tracer-aided modeling in the low-relief, wet-dry tropics suggests water ages and DOC export are driven by seasonal wetlands and deep groundwater. *Water Resour. Res.* 56 (4), e2019WR026175.
- Borah, D.K., Demissie, M., Keefer, L.L., 2002. AGNPS-based assessment of the impact of BMPs on nitrate-nitrogen discharging into an Illinois Water Supply Lake. *Water Int.* 27 (2), 255–265.
- Bourauoi, F., Grizzetti, B., 2011. Long term change of nutrient concentrations of rivers discharging in European seas. *Sci. Total Environ.* 409 (23), 4899–4916.
- Bowes, M.J., Jarvie, H.P., Halliday, S.J., Skeffington, R.A., Wade, A.J., Loewenthal, M., Gozzard, E., Newman, J.R., Palmer-Felgate, E.J., 2015. Characterising phosphorus and nitrate inputs to a rural river using high-frequency concentration-flow relationships. *Sci. Total Environ.* 511, 608–620.

- Boyer, E.W., Hornberger, G.M., Benca, K.E., McKnight, D., 1996. Overview of a simple model describing variation of dissolved organic carbon in an upland catchment. *Ecol. Model.* 86 (2–3), 183–188.
- Carlier, N., 1998. Vers une modélisation hydrologique adaptée à l'évaluation des pollutions diffuses: prise en compte du réseau anthropique. Application au bassin versant de Naizin (Morbihan), Paris. p. 6.
- Casal, L., Durand, P., Akkal-Corfini, N., Benhamou, C., Laurent, F., Salmon-Monviola, J., Vertès, F., 2019a. Optimal location of set-aside areas to reduce nitrogen pollution: a modelling study. *J. Agric. Sci.* 156 (9), 1090–1102.
- Casal, L., Durand, P., Akkal-Corfini, N., Benhamou, C., Laurent, F., Salmon-Monviola, J., Ferrant, S., Probst, A., Probst, J.-L., Vertès, F., 2019b. Reduction of stream nitrate concentrations by land management in contrasted landscapes. *Nutr. Cycl. Agroecosyst.* 114 (1), 1–17.
- Casson, N.J., Eimers, M.C., Watmough, S.A., Richardson, M.C., 2019. The role of wetland coverage within the near-stream zone in predicting of seasonal stream export chemistry from forested headwater catchments. *Hydrol. Process.* 33 (10), 1465–1475.
- Cheverry, C., 1998. Agriculture intensive et qualité des eaux. Editions Quae.
- Davis, C.A., Ward, A.S., Burgin, A.J., Loecke, T.D., Riveros-Iregui, D.A., Schoebelen, D.J., Just, C.L., Thomas, S.A., Weber, L.J., St Clair, M.A., 2014. Antecedent moisture controls on stream nitrate flux in an agricultural watershed. *J. Environ. Qual.* 43 (4), 1494–1503.
- Dick, J.J., Tetzlaff, D., Birkel, C., Soulsby, C., 2014. Modelling landscape controls on dissolved organic carbon sources and fluxes to streams. *Biogeochemistry* 122 (2–3), 361–374.
- Dupas, R., Minaudo, C., Gruau, G., Ruiz, L., Gascuel-Oudou, C., 2018. Multidecadal trajectory of riverine nitrogen and phosphorus dynamics in rural catchments. *Water Resour. Res.* 54 (8), 5327–5340.
- Dusek, J., Dohnal, M., Vogel, T., Marx, A., Barth, J.A., 2019. Modelling multiseasonal preferential transport of dissolved organic carbon in a shallow forest soil: equilibrium versus kinetic sorption. *Hydrol. Process.* 33 (22), 2898–2917.
- Fenicia, F., Savenije, H.H.G., Matgen, P., Pfister, L., 2006. Is the groundwater reservoir linear? Learning from data in hydrological modelling. *Hydrol. Earth Syst. Sci.* 10 (1), 139–150.
- Fenicia, F., Kavetski, D., Savenije, H.H., Clark, M.P., Schoups, G., Pfister, L., Freer, J., 2014. Catchment properties, function, and conceptual model representation: is there a correspondence? *Hydrol. Process.* 28 (4), 2451–2467.
- Ferrant, S., Oehler, F., Durand, P., Ruiz, L., Salmon-Monviola, J., Justes, E., Dugast, P., Probst, A., Probst, J.-L., Sanchez-Perez, J.-M., 2011. Understanding nitrogen transfer dynamics in a small agricultural catchment: comparison of a distributed (TN2T) and a semi distributed (SWAT) modeling approaches. *J. Hydrol.* 406 (1–2), 1–15.
- Ford, W.I., King, K., Williams, M.R., 2018. Upland and in-stream controls on baseflow nutrient dynamics in tile-drained agroecosystem watersheds. *J. Hydrol.* 556, 800–812.
- Fovet, O., Ruiz, L., Fauchoux, M., Molénat, J., Sekhar, M., Vertès, F., Aquilina, L., Gascuel-Oudou, C., Durand, P., 2015. Using long time series of agricultural-derived nitrates for estimating catchment transit times. *J. Hydrol.* 522, 603–617.
- Fovet, O., et al., 2018a. Seasonal variability of stream water quality response to storm events captured using high-frequency and multi-parameter data. *J. Hydrol.* 559, 282–293.
- Fovet, O., et al., 2018b. AgrHyS: an observatory of response times in agro-hydro systems. *Vadose Zone J.* 17 (1), 180066.
- Fuß, T., Behounek, B., Ulseth, A.J., Singer, G.A., 2017. Land use controls stream ecosystem metabolism by shifting dissolved organic matter and nutrient regimes. *Freshw. Biol.* 62 (3), 582–599.
- Godsey, S.E., Kirchner, J.W., Clow, D.W., 2009. Concentration–discharge relationships reflect chemostatic characteristics of US catchments. *Hydrol. Process.* Int. J. 23 (13), 1844–1864.
- Graeber, D., Gelbrecht, J., Pusch, M.T., Anlanger, C., von Schiller, D., 2012. Agriculture has changed the amount and composition of dissolved organic matter in Central European headwater streams. *Sci. Total Environ.* 438, 435–446.
- Gupta, H.V., Kling, H., Yilmaz, K.K., Martinez, G.F., 2009. Decomposition of the mean squared error and NSE performance criteria: implications for improving hydrological modelling. *J. Hydrol.* 377 (1–2), 80–91.
- Harman, C.J., 2015. Time-variable transit time distributions and transport: theory and application to storage-dependent transport of chloride in a watershed. *Water Resour. Res.* 51 (1), 1–30.
- Haygarth, P.M., Jarvie, H.P., Powers, S.M., Sharpley, A.N., Elser, J.J., Shen, J., Peterson, H.M., Chan, N.-L., Howden, N.J., Burt, T., 2014. Sustainable Phosphorus Management and the Need for a Long-term Perspective: The Legacy Hypothesis. ACS Publications.
- Hénault, C., Germon, J., 2000. NEMIS, a predictive model of denitrification on the field scale. *Eur. J. Soil Sci.* 51 (2), 257–270.
- Howden, N.J.K., Burt, T.P., Mathias, S.A., Worrall, F., Whelan, M.J., 2011. Modelling long-term diffuse nitrate pollution at the catchment-scale: data, parameter and epistemic uncertainty. *J. Hydrol.* 403 (3–4), 337–351.
- Hrachowitz, M., Clark, M.P., 2017. HESS opinions: the complementary merits of competing modelling philosophies in hydrology. *Hydrol. Earth Syst. Sci.* 21 (8), 3953–3973.
- Hrachowitz, M., Savenije, H., Bogaard, T., Tetzlaff, D., Soulsby, C., 2013a. What can flux tracking teach us about water age distribution patterns and their temporal dynamics? *Hydrol. Earth Syst. Sci.* 7 (2), 533–564.
- Hrachowitz, M., et al., 2013b. A decade of Predictions in Ungauged Basins (PUB)—a review. *Hydrol. Sci. J.-J. Sci. Hydrol.* 58 (6), 1198–1255.
- Hrachowitz, M., Fovet, O., Ruiz, L., Euser, T., Gharari, S., Nijzink, R., Freer, J., Savenije, H.H.G., Gascuel-Oudou, C., 2014. Process consistency in models: the importance of system signatures, expert knowledge, and process complexity. *Water Resour. Res.* 50 (9), 7445–7469.
- Hrachowitz, M., Fovet, O., Ruiz, L., Savenije, H.H.G., 2015. Transit time distributions, legacy contamination and variability in biogeochemical 1/foscaling: how are hydrological response dynamics linked to water quality at the catchment scale? *Hydrol. Process.* 29 (25), 5241–5256.
- Hrachowitz, M., Benettin, P., Van Breukelen, B.M., Fovet, O., Howden, N.J., Ruiz, L., Van Der Velde, Y., Wade, A.J., 2016. Transit times—the link between hydrology and water quality at the catchment scale. *Wiley Interdiscip. Rev. Water* 3 (5), 629–657.
- Humbert, G., Jaffrezic, A., Fovet, O., Gruau, G., Durand, P., 2015. Dry-season length and runoff control annual variability in stream DOC dynamics in a small, shallow groundwater-dominated agricultural watershed. *Water Resour. Res.* 51 (10), 7860–7877.
- ISO 10304, N., 1995. Determination of Dissolved Fluoride, Chloride, Nitrite, Orthophosphate, Bromide, Nitrate, and Sulfate Ions, Using Liquid Chromatography of Ions (edited by AFNOR).
- Kelleher, C., McGlynn, B., Wagener, T., 2017. Characterizing and reducing equifinality by constraining a distributed catchment model with regional signatures, local observations, and process understanding. *Hydrol. Earth Syst. Sci.* 21 (7), 3325.
- Knoben, W.J., Freer, J.E., Woods, R.A., 2019. Inherent benchmark or not? Comparing Nash–Sutcliffe and Kling–Gupta efficiency scores. *Hydrol. Earth Syst. Sci.* 23 (10), 4323–4331.
- Lambert, T., Pierson-Wickmann, A.-C., Gruau, G., Jaffrezic, A., Petitjean, P., Thibault, J.-N., Jeanneau, L., 2013. Hydrologically driven seasonal changes in the sources and production mechanisms of dissolved organic carbon in a small lowland catchment. *Water Resour. Res.* 49 (9), 5792–5803.
- Lambert, T., Pierson-Wickmann, A.C., Gruau, G., Jaffrezic, A., Petitjean, P., Thibault, J.N., Jeanneau, L., 2014. DOC sources and DOC transport pathways in a small headwater catchment as revealed by carbon isotope fluctuation during storm events. *Biogeosciences* 11 (11), 3043–3056.
- Lee, K.-Y., Fisher, T.R., Jordan, T.E., Correll, D.L., Weller, D.E., 2000. Modeling the hydrochemistry of the Choptank River Basin using GWLF and Arc/Info: 1. Model calibration and validation. *Biogeochemistry* 49 (2), 143–173.
- Lindström, G., Pers, C., Rosberg, J., Strömqvist, J., Arheimer, B., 2010. Development and testing of the HYPE (Hydrological Predictions for the Environment) water quality model for different spatial scales. *Hydrol. Res.* 41 (3–4), 295–319.
- Medici, C., Wade, A.J., Francés, F., 2012. Does increased hydrochemical model complexity decrease robustness? *J. Hydrol.* 440–441, 1–13.
- Molénat, J., Gascuel-Oudou, C., Davy, P., Durand, P., 2005. How to model shallow water-table depth variations: the case of the Kervidy-Naizin catchment, France. *Hydrol. Process.* Int. J. 19 (4), 901–920.
- Molénat, J., Gascuel-Oudou, C., Ruiz, L., Gruau, G., 2008. Role of water table dynamics on stream nitrate export and concentration in agricultural headwater catchment (France). *J. Hydrol.* 348 (3–4), 363–378.
- Montreuil, O., Merot, P., Marmonier, P., 2010. Estimation of nitrate removal by riparian wetlands and streams in agricultural catchments: effect of discharge and stream order. *Freshw. Biol.* 55 (11), 2305–2318.
- Morel, B., Durand, P., Jaffrezic, A., Gruau, G., Molenat, J., 2009. Sources of dissolved organic carbon during stormflow in a headwater agricultural catchment. *Hydrol. Process.* 23 (10), 2888–2901.
- Musolf, A., Schmidt, C., Rode, M., Lischeid, G., Weise, S.M., Fleckenstein, J.H., 2016. Groundwater head controls nitrate export from an agricultural lowland catchment. *Adv. Water Resour.* 96, 95–107.
- Oehler, F., Durand, P., Bordenave, P., Saadi, Z., Salmon-Monviola, J., 2009. Modelling denitrification at the catchment scale. *Sci. Total Environ.* 407 (5), 1726–1737.
- Outram, F.N., et al., 2014. High-frequency monitoring of nitrogen and phosphorus response in three rural catchments to the end of the 2011–2012 drought in England. *Hydrol. Earth Syst. Sci.* 18 (9), 3429–3448.
- Outram, F.N., Cooper, R.J., Sunnenberg, G., Hiscock, K.M., Lovett, A.A., 2016. Antecedent conditions, hydrological connectivity and anthropogenic inputs: factors affecting nitrate and phosphorus transfers to agricultural headwater streams. *Sci. Total Environ.* 545–546, 184–199.
- Penman, H.L., 1956. Estimating evaporation. *Trans. Am. Geophys. Union* 37 (1), 43.
- Petitjean, P., Henin, O., Gruau, G., 2004. Dosage du carbone organique dissous dans les eaux douces naturelles. Intérêt, Principe, Mise en Oeuvre et Précautions Opératoires.
- Pettersson, A., Arheimer, B., Johansson, B., 2001. Nitrogen concentrations simulated with HBV-N: new response function and calibration strategy - paper presented at the Nordic Hydrological Conference (Uppsala, Sweden June, 2000). *Nord. Hydrol.* 32 (3), 227–248.
- Rinaldo, A., Benettin, P., Harman, C.J., Hrachowitz, M., McGuire, K.J., Van Der Velde, Y., Bertuzzo, E., Botter, G., 2015. Storage selection functions: a coherent framework for quantifying how catchments store and release water and solutes. *Water Resour. Res.* 51 (6), 4840–4847.
- Seibert, J., Grabs, T., Köhler, S., Laudon, H., Winterdahl, M., Bishop, K., 2009. Linking soil- and stream-water chemistry based on a riparian flow-concentration integration model. *Hydrol. Earth Syst. Sci.* 13 (12), 2287–2297.
- Shafiq, M., Craig, J.R., Macrae, M.L., English, M.C., Schiff, S.L., Van Cappellen, P., Basu, N.B., 2019. Can improved flow partitioning in hydrologic models increase biogeochemical predictability? *Water Resour. Res.* 55 (4), 2939–2960.
- Shrestha, R.R., Osenbrück, K., Rode, M., 2013. Assessment of catchment response and calibration of a hydrological model using high-frequency discharge–nitrate concentration data. *Hydrol. Res.* 44 (6), 995–1012.
- Smith, A.P., Western, A.W., Hannah, M.C., 2013. Linking water quality trends with land use intensification in dairy farming catchments. *J. Hydrol.* 476, 1–12.
- Strohmeier, L., Fovet, O., Akkal-Corfini, N., Dupas, R., Durand, P., Fauchoux, M., Gruau, G., Hamon, Y., Jaffrezic, A., Minaudo, C., 2020. Multi-temporal relationships between the hydro-climate and exports of carbon, nitrogen and phosphorus in a small agricultural watershed. *Water Resour. Res.* 56 (7), e2019WR026323.

- Taylor, P.G., Townsend, A.R., 2010. Stoichiometric control of organic carbon-nitrate relationships from soils to the sea. *Nature* 464 (7292), 1178–1181.
- Thomas, Z., Abbott, B.W., Troccaz, O., Baudry, J., Pinay, G., 2016. Proximate and ultimate controls on carbon and nutrient dynamics of small agricultural catchments. *Biogeosciences* 13 (6), 1863–1875.
- Thompson, S., Basu, N., Lascourain, J., Aubeneau, A., Rao, P., 2011. Relative dominance of hydrologic versus biogeochemical factors on solute export across impact gradients. *Water Resour. Res.* 47 (10).
- Trevisan, D., Giguët-Covex, C., Sabatier, P., Quetin, P., Arnaud, F., 2019. Coupling indicators and lumped-parameter modeling to assess suspended matter and soluble phosphorus losses. *Sci. Total Environ.* 650 (Pt 2), 3027–3040.
- Viaud, V., Santillán-Carvantes, P., Akkal-Corfini, N., Le Guillou, C., Prévost-Bouré, N.C., Ranjard, L., Menasseri-Aubry, S., 2018. Landscape-scale analysis of cropping system effects on soil quality in a context of crop-livestock farming. *Agric. Ecosyst. Environ.* 265, 166–177.
- Whitehead, P., Wilson, E., Butterfield, D., Seed, K., 1998. A semi-distributed integrated flow and nitrogen model for multiple source assessment in catchments (INCA): part II—application to large river basins in south Wales and eastern England. *Sci. Total Environ.* 210, 559–583.
- Woodward, S.J.R., Stenger, R., 2018. Bayesian chemistry-assisted hydrograph separation (BACH) and nutrient load partitioning from monthly stream phosphorus and nitrogen concentrations. *Stoch. Environ. Res. Risk Assess.* 32 (12), 3475–3501.
- Woodward, S.J.R., Stenger, R., Bidwell, V.J., 2013. Dynamic analysis of stream flow and water chemistry to infer subsurface water and nitrate fluxes in a lowland dairying catchment. *J. Hydrol.* 505, 299–311.
- WRB, I.W.G., 2006. World Reference Base for Soil Resources. edited. Food and Agriculture Organization (FAO) Rome, Italy, pp. 1–128.
- Xu, N., Saiers, J.E., Wilson, H.F., Raymond, P.A., 2012. Simulating streamflow and dissolved organic matter export from a forested watershed. *Water Resour. Res.* 48 (5), 18.
- Zuecco, G., Penna, D., Borga, M., van Meerveld, H.J., 2016. A versatile index to characterize hysteresis between hydrological variables at the runoff event timescale. *Hydrol. Process.* 30 (9), 1449–1466.